Detection of Cracks in Shafts via Analysis of Vibrations and Orbital Paths

R. Peretz[1], L. Rogel[2], J. Bortman[3], and R. Klein[4]

[1,2,3]*Pearlstone Center for Aeronautical Engineering Studies and Laboratory for Mechanical Health Monitoring, Department of Mechanical Engineering, Ben-Gurion University of the Negev, P.O. Box 653, Beer Sheva 8410501, Israel*

refaelpe@post.bgu.ac.il
rogell@post.bgu.ac.il
jacbort@bgu.ac.il

[4]*R.K. Diagnostics, P.O. Box 101, Gilon, D.N. Misgav 20103, Israel*
renata.klein@rkdiagnostics.co.il

ABSTRACT

Shafts are often subjected to difficult operating conditions in high-performance rotating equipment such as compressors, steam and gas turbines, generators and pumps. As a result, shafts are susceptible to fatigue failures due to transverse cracks. In this study, vibration monitoring and orbital paths observation were used to detect the presence of a flaw in a shaft. Two types of flaws were tested: a straight slot, and a fatigue crack. For both flaw types, specimens of different depths were examined in order to assess the detection capability. A new approach to examine vibrations at the critical speed is proposed; this speed is chosen because of the strong connection to the basics of the physical problem. Orbital paths are suggested as means for fault detection as well. The presence of a straight slot in the shaft was found to be related to a decrease in the natural frequency and to a decrease in amplitude of the first order at critical speed. For the fatigue crack, a consistent trend in critical speed and in amplitude was not seen as crack depth grew. A new method to detect the change in the shaft natural frequency is proposed. The combination of two indicators, change in critical speed and change in amplitude at critical speed, are suggested for classification of flaw size. For the straight slot case, the method proposed was able to distinguish between different fault depths.

1. INTRODUCTION

Shafts are components subjected to difficult operating conditions in high-performance rotating equipment such as compressors, steam and gas turbines, generators and pumps.

Many rotor dynamic systems contain shafts that are susceptible to fatigue failure due to transverse cracks, cracks in the shaft which grow perpendicular to the shaft axis. A transverse crack occurs due to the fatigue of the shaft material because of excessive bending moment. Formation and propagation of cracks in rotors represent a fundamental problem not only for the safety, but also for the operating and manufacturing costs which are involved in the substitution of the rotor.

Cracked rotating shafts have been the object of studies and investigations since the 1970s (Wauer, 1990). An early detection of a crack can considerably extend the durability of rotating machineries, thus increasing their uptime and safety. Vibration monitoring is one approach for detecting cracks that could be implemented in an automated manner and can be conducted without disturbing the machinery operation. Crack detection in rotating shafts (during operation) remains a difficult problem; a reliable method for crack detection has yet to be found.

It is known that the presence of faults somewhat alters the vibrational characteristics of rotor dynamic systems, and therefore, those variations have often been used to detect damage in rotating machinery. Theoretical models predict variations such as: increase in amplitude of the first, second and third order of speed frequency and decrease in natural frequency. Also, an elevation in amplitude at half and third of critical speed have been reported. Some changes are attributed to the decrease in the shaft stiffness due to the presence of the crack, others due to crack opening and closing. Another method reported is observation of the rotor orbitals which vary with crack presence. Some of these characteristics have been tested experimentally as well. The effectiveness of each method is proportional to the crack depth (Dimarogonas, 1996; Sabnavis, Kirk, Kasarda & Quinn, 2004; Sinou & Lees, 2007; Sinou, 2008; Machorro-

López, Adams, Gómez-Mancilla & Gul, 2009; AL-Shudeifat, Butcher & Stern, 2010; Varney & Green, 2012).

Sinou & Lees (2007) addressed the influence of crack opening and closing on dynamic response during operation. In their model, the breathing crack is evaluated by expanding the changing stiffness of the crack as a truncated Fourier series and then using the Harmonic Balance Method. After conducting a parametric study they concluded that both the orbit evolution at half of the first critical speed, and the magnitude of the response at the first critical speed and at half of the first critical speed may be considered as the unique characteristics of the system responses with a breathing crack and also served as target observations for monitoring rotating machinery.

Suryawanshi & Dhamande, (2014) conducted experimental investigations of the effects of cracks and damages on the integrity of structures, with a view to detect, quantify their effect by identifying some parameter such as critical speed and RMS velocity.

Kunche & Ganeriwala (2013) performed a series of tests on a SpectraQuest Machinery Fault Simulator with cracked shafts to observe their behavioral changes, including the critical speed, 1X, 2X and higher harmonics frequency responses, compared with an intact shaft. A special emphasis was placed on determining a unique distinguishing signature of shaft crack that could be used for monitoring the health of rotating machinery. The results show that the critical speed decreased as the crack increased, and the 1X and 2X frequency response for cracked shaft increased compared with the intact shaft.

Machorro-López et al. (2009) recommend use of external excitation with piezoelectric actuators. They developed a detailed physics-based three-dimensional model of an experimental Machinery Fault Simulators apparatus using ANSYS® with beam elements based on Timoshenko beam theory. Different kinds of faults such as transverse cracks, imbalance, misalignment, bent shafts, and combinations were considered. Numerical and experimental results showed that the natural frequencies and mode shapes do not vary significantly when a transverse crack appears in the shaft of a rotordynamic system; therefore, active sensing is necessary to detect the damage.

In their paper, Machorro-López et al. (2009) discuss the variety of opinions on several crack detection methods: "The specific case of cracks in rotating shafts is more difficult to diagnose. There is no general agreement regarding the characteristic vibratory tendencies of this kind of damage. Some researchers report that changes in natural frequencies and/or mode shapes can be used to detect cracks, whereas other researchers report contradictory findings. Many researchers have proposed the vibration amplitudes at the 1X and/or 2X frequency components as indicators of cracks in shafts, but other many researchers

disagree with this proposal, indicating that imbalance and misalignment are common faults whose effects are more evident at those frequency components, thereby masking the crack. Similarly, a group of researchers has presented techniques for crack detection by analyzing the peaks of vibratory amplitudes occurring at higher frequency components (3X, 4X, etc.); however, another group reports that these amplitudes are highly damped; consequently, the high-frequency amplitudes are too small, making it difficult to detect the crack."

Many theoretical models appear in the literature, some partially validated by experiments, yet still there exists a lack of sufficient experimental studies and cases. Amount of diversification or robustness of the experimental work reported is usually overlooked. In this study, an experimental investigation is performed to validate several detection methods and to propose a consolidated detection method. Vibration monitoring and orbital observation are used to detect the presence of a flaw in a shaft. In particular analysis of slow accelerations and decelerations by trending of: vibration RMS, first order tracking and orbital paths. The methods chosen are passive and do not require intervention with the monitored system, an advantage for industrial machines.

2. EXPERIMENTAL SETUP

The experimental apparatus comprises of a shaft and two disks placed a third distance from the bearings, see Figure 1. The shaft diameter is 20mm, the length between the bearings is 470mm and the mass of each disk is 10.5kg. At the center of the shaft, two types of flaws are tested: the first, a straight slot, and the second a fatigue crack. In both cases specimens of different depths were examined. The flaws tested are presented in Table 1. Measurements were taken by triaxial accelerometers, proximity sensors and a magnetic sensor (for shaft speed). A triaxial accelerometer was placed on the top of each bearing house. The proximity sensors monitored the movement of one of the disks in the horizontal and vertical directions. The magnetic sensor measured the shaft speed.

2.1. Creation of the Flaws

The straight slot flaws were created in the shafts by a disk of 0.3mm width. The flaw ending in the shaft is a straight line. The depth of the flaw presented in Table 1 indicates the perpendicular distance between the flaw end to the diameter.

The fatigue cracks were created by means of a three point bending scheme. An initial notch of 1.35mm depth was made in order to rule the location of crack growth. Crack size and shape in the shaft is unknown, however, the extension of the crack on the shaft circumference was measured by means of a light microscope. The depth of the flaw mentioned in Table 1 refers to the crack length on the surface.

Pictures of the flaws created are presented in Figure 2.

2.2. Experiment Procedure

The testing of a shaft requires dismantling and reassembling of the test rig. In order to reduce the amount of misalignment, a commercial SKF laser system was used.

Recordings were taken at shaft speed varying from 10Hz to 50Hz. This range was chosen to include the first natural frequency of the shaft and disks. A simplified modal analysis is presented in the Appendix. The purpose of this sweep is to find the critical speed of the system in order to examine possible fault indicators at that speed. Measurements were taken for acceleration and deceleration of the shaft, five recordings each, a total of ten recordings for each shaft. Each recording took seven minutes and was performed at a sampling rate of 25,000Hz. The rate of acceleration and deceleration was chosen as the minimum possible by the controller in order to perform a quasi-steady state sweep. This procedure was repeated for all ten shafts.

Table 1. Flaws examined in the experiment.

Flaw type	Shaft #	Flaw depth
Straight slot (open crack)	slot 1	0 (Healthy)
	slot 2	4 mm
	slot 3	6 mm
	slot 4	8 mm
Fatigue crack	fatigue 1	1.35 mm (only notch)
	fatigue 2	1.35+0.95=2.3 mm
	fatigue 3	1.35+3.65=5 mm
	fatigue 4	1.35+4.05=5.4 mm
	fatigue 5	1.35+5.8=7.15 mm
	fatigue 6	1.35+7.55=8.9 mm
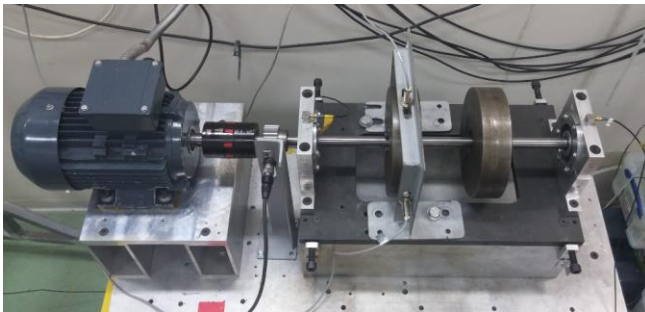
Figure 1. Experimental setup.
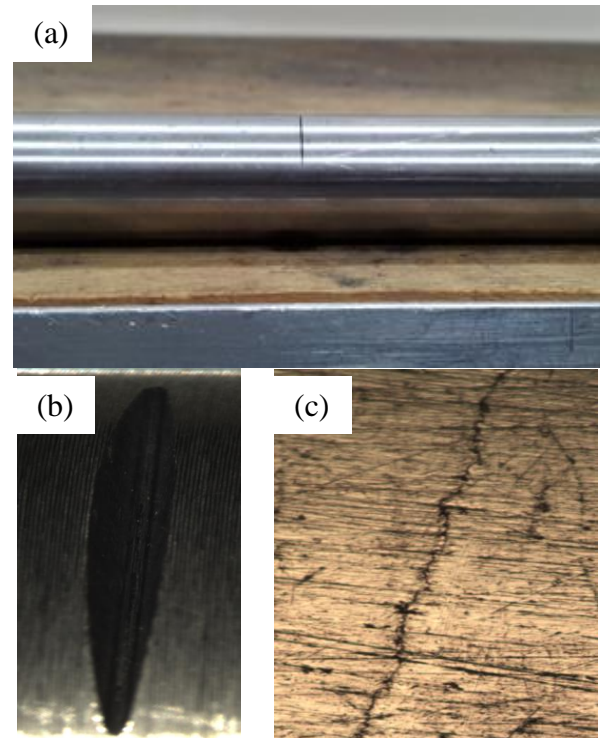
Figure 2. Flaws created in the shafts, (a) straight slot (b) initial notch for fatigue crack growth (c) the crack on shaft circumference as seen through a light microscope.

3. METHODS OF ANALYSIS

The post-processing performed on the signals measured is elaborated in this chapter.

3.1. Acceleration Signals

The acceleration signals were analyzed in the order domain, order tracking specifically. The vibration measurements are resampled according to the shaft speed, which is deciphered from the magnetic sensor. The resampled data is divided into segments containing 160 cycles with 50% overlap. Each segment is transformed to the order domain composing a spectrogram matrix of vibration levels as function of the shaft speed (RPS) and the order. Based on the vibration levels at the first order the critical speed is determined as the frequency with highest amplitude. The result is a graph of the amplitude at the first order vs. shaft speed. The processing scheme is presented in Figure 3.
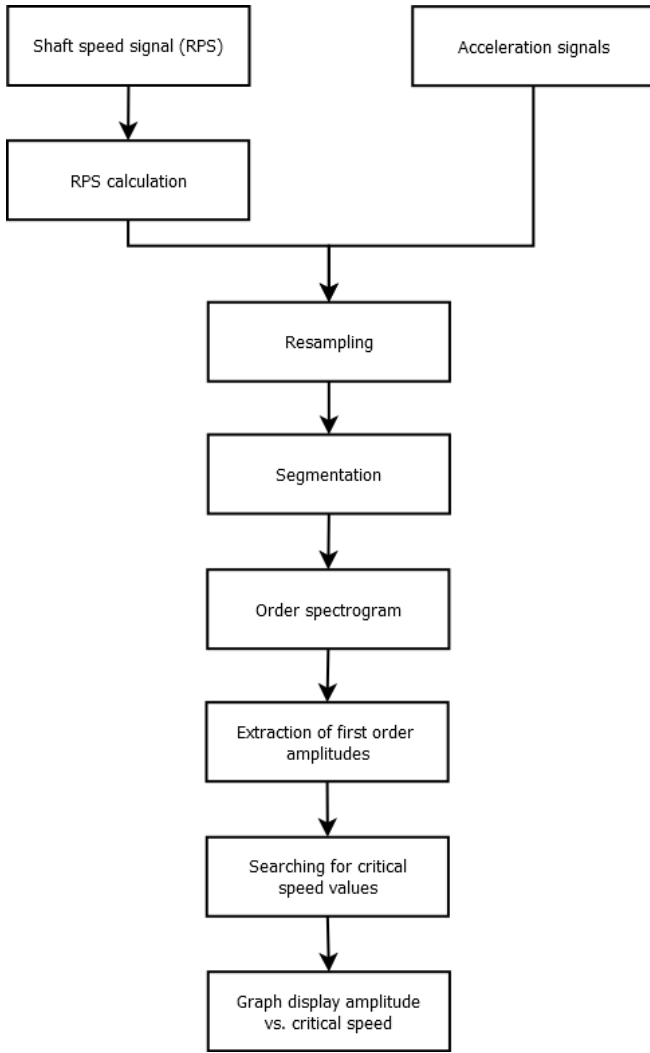
Figure 3. Processing scheme for acceleration signals.

3.2. Proximity Signals – Orbital Paths

Two proximity sensors are monitoring the movement of the center of one of the disks while shaft speed is accelerated and decelerated. The acceleration rate was chosen as minimum as possible to obtain quasi-steady state speeds for the shaft. The processing scheme is presented in Figure 4.

4. ACCELERATION RESULTS

The results of the analysis for each type of flaw are presented by three types of graphs on which all measurements are plotted:

a. Amplitude at critical speed vs. critical speed. This graph shows the change in critical speed and amplitude for different flaw depths, as well as the variation of the repetitions.

b. Order tracking. Unlike the first graph which gives information at one speed value, in this graph behavior and trends along the tested speed range is shown.

c. Critical speed vs. flaw depth.
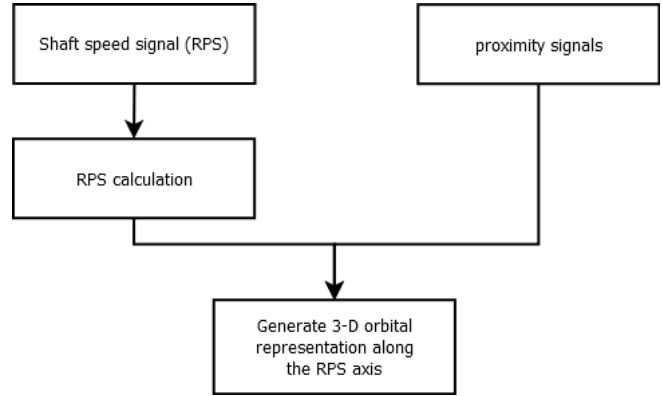
Figure 4. Processing scheme for proximity signals.

4.1. Straight Slot (Open Crack)
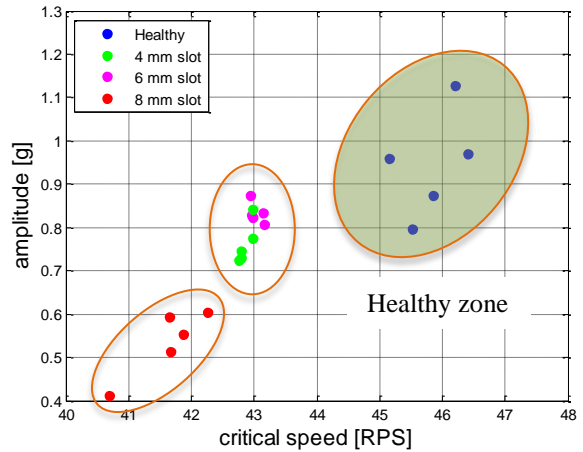
Figure 5. Amplitude at critical speed vs. critical speed for the straight slot flaw type. Three distinct groups of flaw depths are seen: healthy, 4-6 mm and 8 mm.
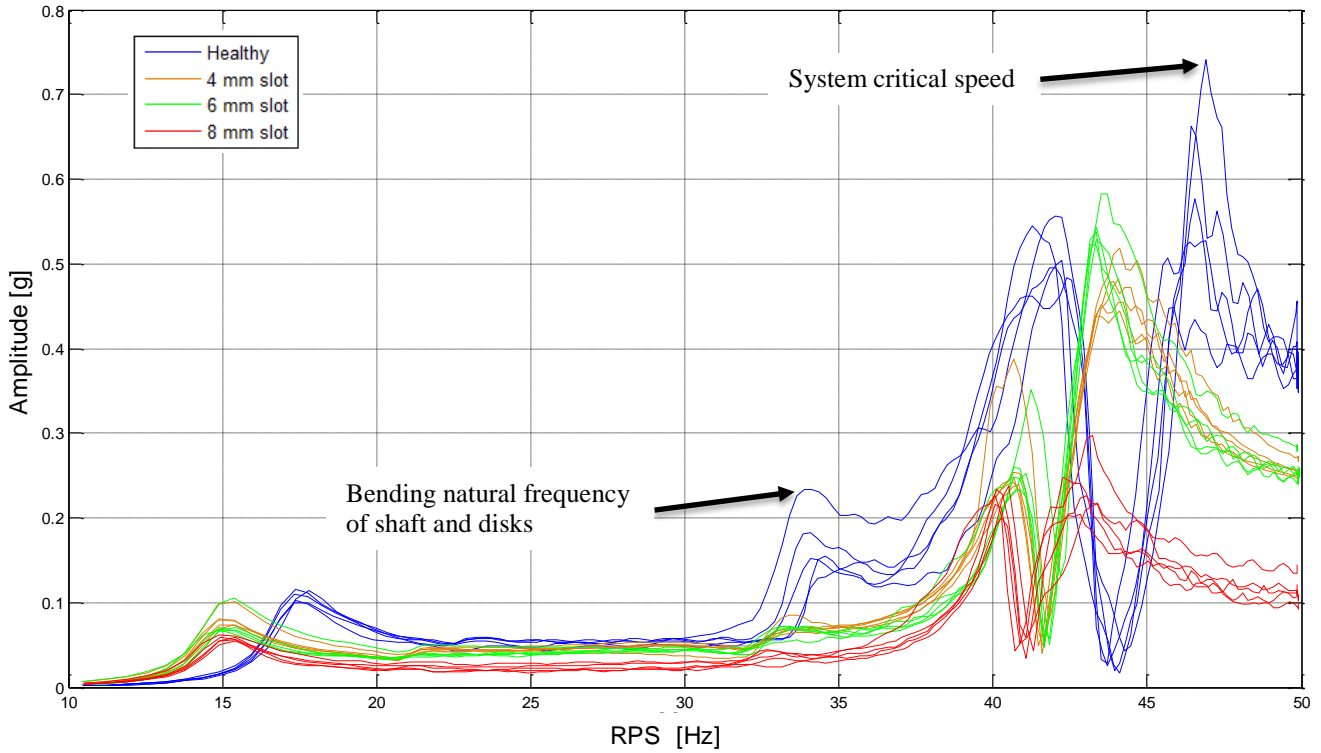
Figure 6. First order vs. RPS during acceleration for straight slot flaw type.
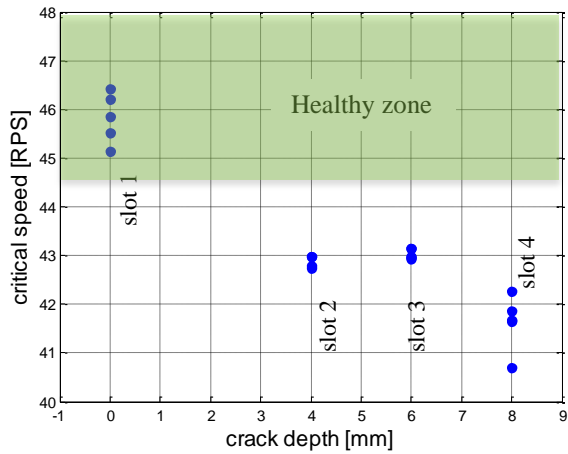
Figure 7. Critical speed vs. flaw depth for the straight slot flaw type, acceleration.

From the graphs shown, the following remarks may be made:

- A clear distinction is seen between the healthy shaft and a flawed shaft, by means of change in critical speed and by means of change in amplitude. In both cases a decrease in value is

observed between the healthy and flawed shafts. This is best seen in Figure 5.
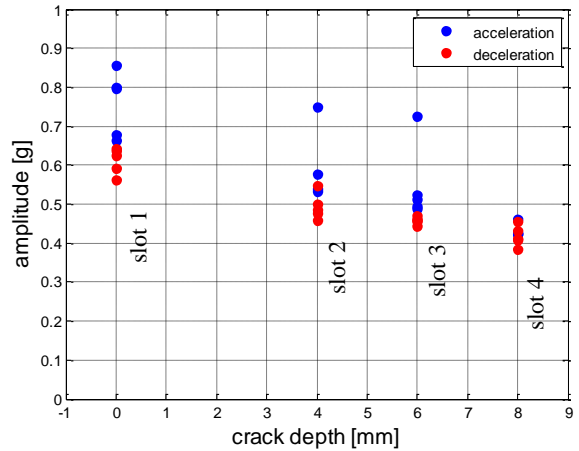
Figure 8. Amplitude at critical speed vs. crack depth for straight slot flaw type.

- Critical speed and amplitude at critical speed decrease as flaw depth grows. The combination of decrease in critical speed and decrease in amplitude allows classification of the shafts into three groups:

5

healthy, flaw depth 4-6 mm and flaw depth 8 mm (see Figure 5).

- In Figures 5 and 6, a decrease in amplitude is observed with growth of flaw depth. This behavior is seen along the entire speed range tested and not only at the critical speed. This may occur if the damping of the system increases as the flaw grows in size. One possible explanation is that as the flaw grows the deflection of the shaft increases as well. This bending adds friction to the bearing which in turn increases the damping in the system. Another possible explanation is that the bending causes the disks to tilt out of their original plane and in turn they resist due to angular momentum, thus adding fictive damping to the system.

- In Figure 7 a clear distinction is seen between the healthy shaft and a flawed shaft, by means of change in critical speed. A decrease in critical speed is seen with increase in flaw depth.

- In Figure 8 a hysteresis is observed between acceleration and deceleration. Although the difference, the same conclusions may be drawn from either trend.

- In Figure 6 a peak is observed at the bending natural frequency of the shaft and disks system

($\approx$34.8Hz), as predicted by a simplified modal analysis (Appendix) for the healthy shaft. This peak is lowered as the flaw grows due to increase in the system damping, as explained earlier.

4.2. Fatigue Crack
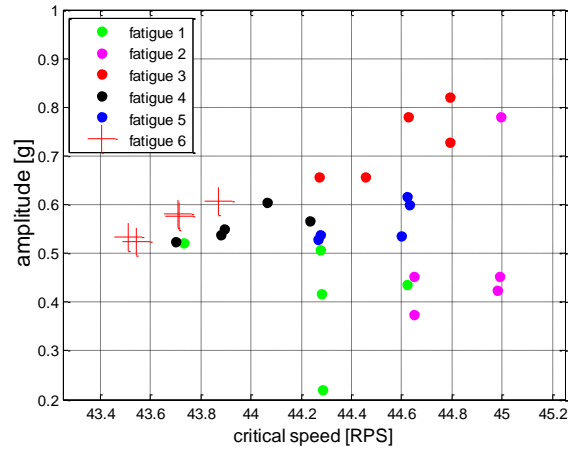
Figure 9. Amplitude at critical speed vs. critical speed for the fatigue crack flaw type.
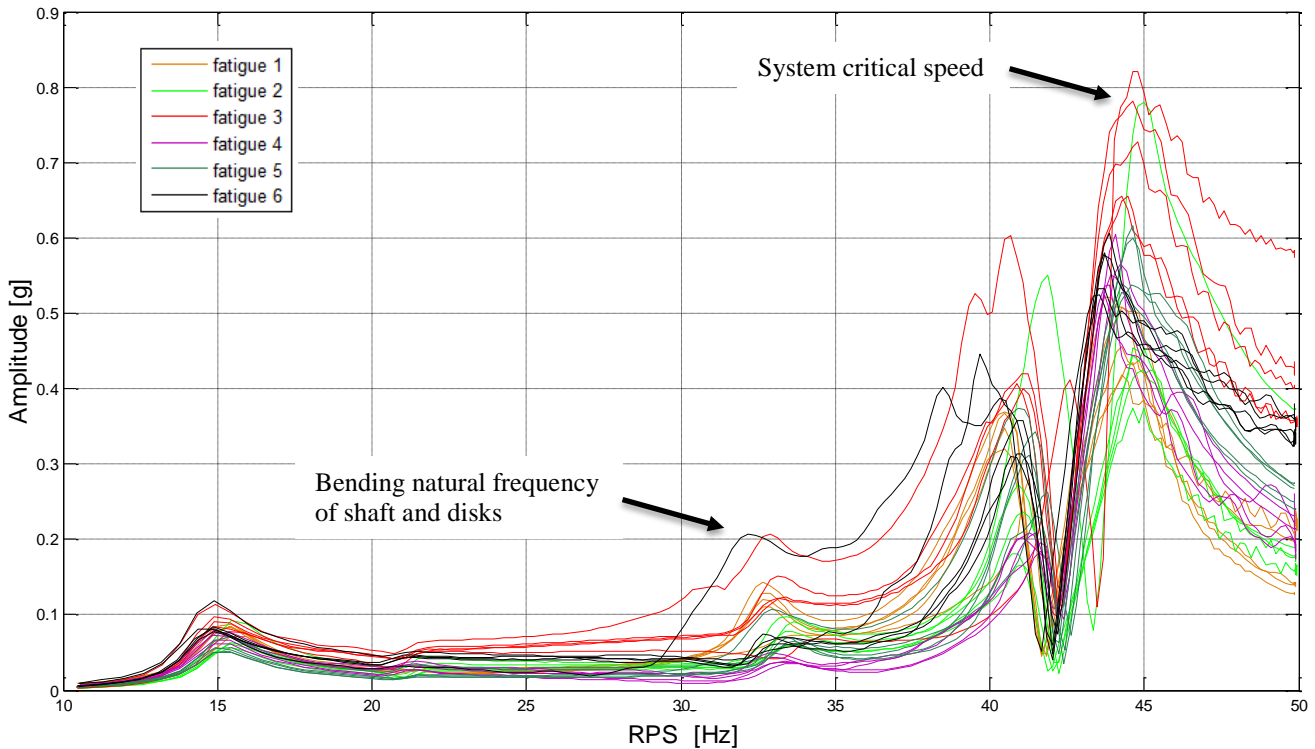
Figure 10. First order vs. RPS during acceleration for fatigue crack flaw type.
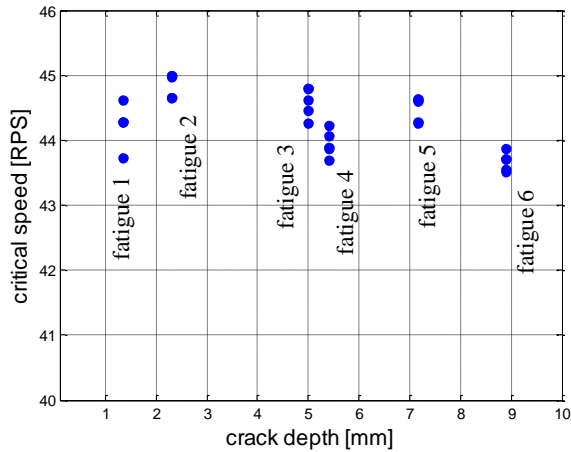
Figure 11. Critical speed vs. crack depth for fatigue crack flaw type.

For the fatigue crack, the results are not conclusive. From the graphs, Figures 9 to 11, a consistent trend in critical speed and in amplitude was not seen as crack depth grew. One possible reason for this outcome is that the influence of the initial notch, used for crack growth, masks the breathing crack behavior. Comparison was made to a shaft with an initial notch only ("fatigue 1") in attempt to discriminate between the flaw types, however the analysis performed may not be sensitive enough for fatigue crack detection. Another explanation might be the crack closure effect. Gudmundson (1983) investigated, numerically and experimentally, open cracks and fatigue cracks in beams. The crack closure effect was experimentally investigated for an edge-cracked beam with a fatigue crack. He found that the eigenfrequencies decreased, as functions of crack length, at a much slower rate than in the case of an open crack. The experimental investigation of the crack closure effect in a vibrating beam showed that this effect is of considerable importance. The residual stresses, which result from the crack growth, act to close the crack. Thus, for small vibrational amplitudes the crack will not open and no changes in the eigenfrequencies are observed.

5. PROXIMITY SIGNALS RESULTS – ORBITAL PATHS

The orbital paths provide complementary observations, to the acceleration signals, in respect to flaw detection. The evolution of orbital paths as the shaft accelerates is presented in Figure 12 for the two cases examined, straight slot and fatigue crack. Growth of the orbital radius is seen with increase in speed. As shaft speed passes through the critical speed and through the bending natural frequency of the shaft and disks system an increase in orbital paths is observed. After passing those speeds the orbit decreases, see Figure 13 and Figure 14 for top and side view of the orbits. Passage of these speeds is accompanied by change in amplitude, phase and shape of the orbit. Visual differences

may be seen between the orbit evolution for the two types of flaws. Finding reliable indicators, which may quantify changes in orbits in relation to flaw depth and type, will be the focus of future research.
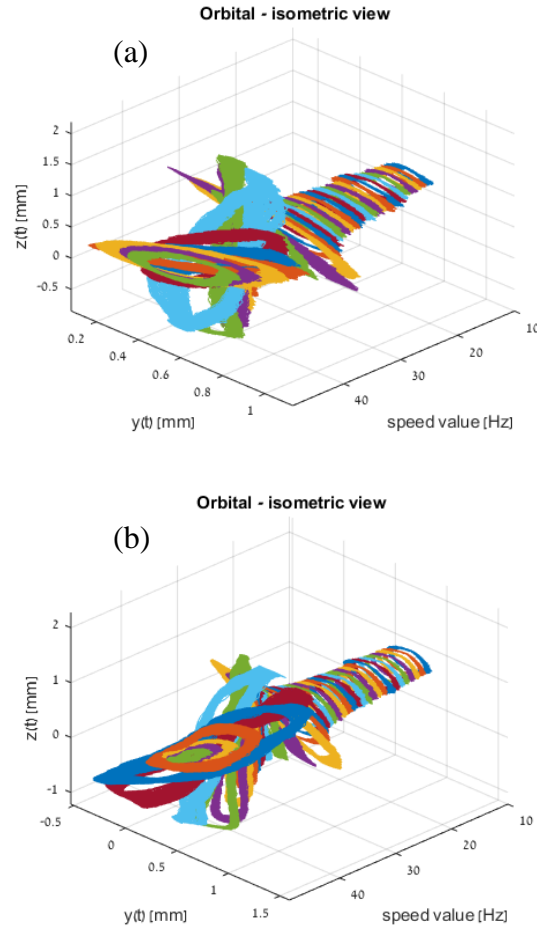
Figure 12. Example of isometric view on orbital paths along the tested speed range, (a) straight slot (b) fatigue crack. Each color represents an orbit at a different speed value, every 1Hz, (y – horizontal displacement, z – vertical displacement).

5.1. Straight Slot Observations

In order to aid in the visualization of the orbit evolution and in order to observe flaw depth effect on behavior, top and side views of the orbital paths are drawn, Figures 13 and 14 respectively. In these views, the same remarks as from the acceleration signals are obtained:

- In the top view of the orbital paths, Figure 13, peaks are seen at two speeds, one at the system critical speed (46Hz) and another at the shaft and disks subsystem's bending critical speed (≈34Hz). The values are for the healthy shaft.

- In Figures 13 and 14 a clear distinction is seen between the healthy shaft and a flawed shaft, by means of change in critical speed.

- Consistency of the results was seen between repetitions.

- The observations made are consistent with the results obtained from the acceleration signals.

Additional remarks, seen from the orbital paths are:

- In the side view of the orbital paths, Figure 14, a peak at speed 43Hz is seen for the healthy shaft. A decrease of this value is seen for the flawed shafts, which distinguishes them from the healthy shaft but not between themselves.

- For the largest flaw, a peak at half the system critical speed is observed at the side view, Figure 14.

5.2. Fatigue Crack Observations

As for the acceleration signals, for the fatigue crack, difficulty in distinction between flaw depths was encountered also in the orbital paths. Change in critical speed was examined, where no distinct decrease was seen. The observations made are inconsistent. In the orbital paths a peak at half the system critical speed was observed in the side view for all the shafts. For the straight slot flaw type this occurred only for the largest flaw. However, since the fatigue cracks encompass an initial notch, which was used for crack growth, it is hard to say whether this peak is related to the cracks or to the presence of the notch.

6. SUMMARY

Crack detection in rotating shafts (during operation) is investigated by many researchers, still, a reliable method for crack detection has yet to be found. Fault diagnostics in shafts remains a difficult problem for laboratory testbeds,
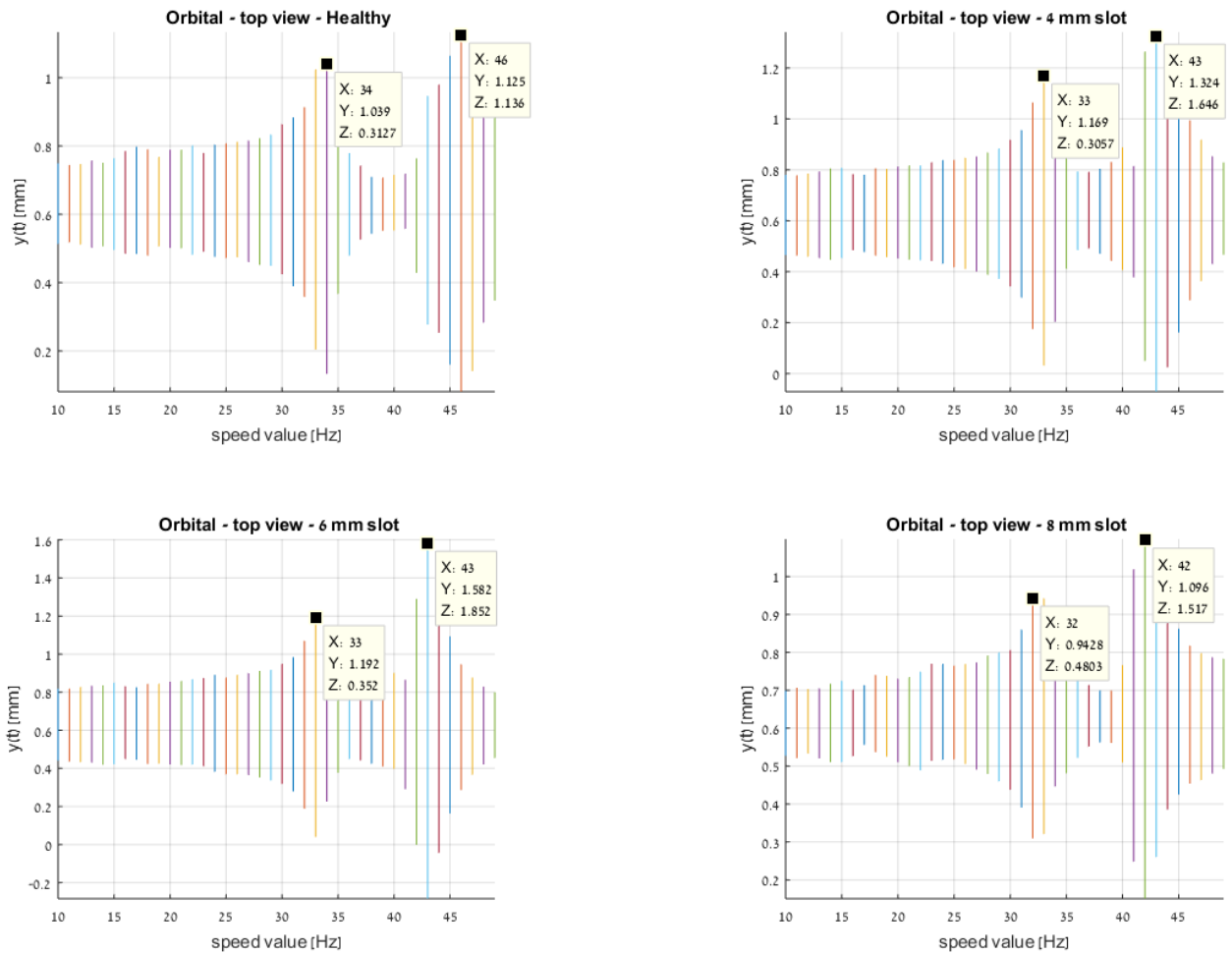
Figure 13. Top view on orbital paths along the tested speed range, acceleration.
y – horizontal displacement
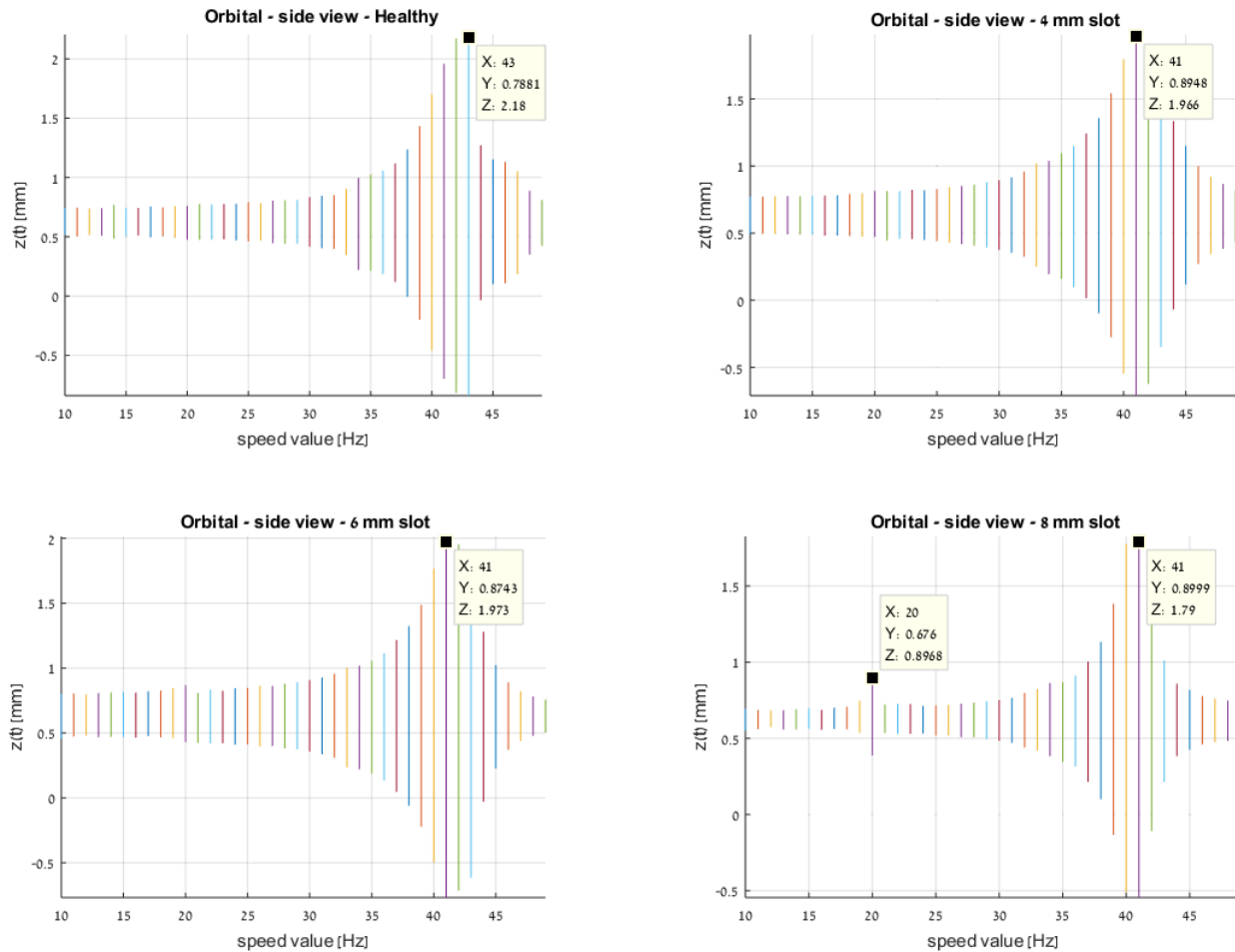
Figure 14. Side view on orbital paths along the tested speed range, acceleration.
z – vertical displacement

which is further complicated in industrial machines. In this study, vibration monitoring and orbital paths observation were used to detect the presence of a flaw in a shaft. Two types of flaws were tested: a straight slot, and a fatigue crack. For both flaw types, specimens of different depths were examined in order to assess the detection capability. Amplitude at critical speed and the critical speed were examined as flaw indicators. This speed was chosen because of the strong connection to the basics of the physical problem. The critical speed was extracted from experiments with rotating speed sweeping from 10 to 50 Hz. Hysteresis was observed between acceleration and deceleration. Still, the same trends and remarks were seen either way. Shafts can be monitored and their maintenance scheduled by implementing the proposed method on periodic accelerations or decelerations of the rotor speed.

For the straight slot flaw type, distinction between a healthy shaft and a flawed shaft was made. Furthermore, the combination of amplitude at critical speed and change in critical speed allowed the classification of the shafts into three groups depending on flaw depths; healthy, flaws of 4-6 mm depth and flaws of 8 mm depth. This method of classification may be preferable for flaw diagnostics since amplitude is also affected by other phenomena such as unbalance and misalignment. Visual observation of orbital paths evolution at the tested speed range concluded in similar remarks. Search for reliable indicators, which may quantify changes in orbits related to flaw depth and type, is planned for further analysis. Some of the possible indicators are amplitude, phase and shape (asymmetry of orbit).

For the fatigue crack flaw type, a distinction of flaw depths was not possible. The acceleration signals did not reveal a consistent trend in critical speed and in amplitude as crack depth grew. One possible reason for this outcome is that the influence of the initial notch, used for crack growth, masks the breathing crack behavior.

7. CONCLUSIONS

The main conclusions of this work are:

9

- The open crack is clearly detectable both by change in critical speed and by vibrations amplitude decrease at critical speed. The results were consistent in vibrations measured during accelerations and decelerations of the rotating speed.

- For the open crack, clear decreasing trends were observed in amplitude of vibrations at critical speed with increase of flaw depth. Decreasing trends of the critical speed with crack depth growth were also observable. The combination of amplitude at critical speed and change in critical speed allowed the classification of the shafts depending on flaw depths. A first step towards prognostics was made.

- For the fatigue crack, a distinction of flaw depths was not possible. The acceleration signals did not reveal a consistent trend in critical speed and in amplitude as crack depth grew.

- The orbit paths analysis was only qualitative. It may provide valuable insights. Therefore, search for reliable indicators, which may quantify changes in orbits related to flaw depth and type, is planned for further analysis.

- The main achievement of this study is successful classification of open crack depth using advanced methods of vibration analysis.

REFERENCES

AL-Shudeifat, M. A., Butcher, E. A., & Stern, C. R. (2010). General harmonic balance solution of a cracked rotor-bearing-disk system for harmonic and sub-harmonic analysis: Analytical and experimental approach. *International Journal of Engineering Science*, 48(10), 921-935. doi:10.1016/j.ijengsci.2010.05.012

Budynas, R. G., & Nisbett, J. K. (2011). Shigley's mechanical engineering design: Ninth edition. New York, NY: McGraw-Hill.

Dimarogonas, A. D. (1996). Vibration of cracked structures: a state of the art review. *Engineering fracture mechanics*, 55(5), 831-857.

Gudmundson, P. (1983). The dynamic behaviour of slender structures with cross-sectional cracks. *Journal of the Mechanics and Physics of Solids*, 31(4), 329-345. doi:10.1016/0022-5096(83)90003-0

Kunche, S., & Ganeriwala, S. N. S (2013). The Effect of Unbalance and Misalignment on Detection of Rotor/Shaft Cracks Using Vibration Analysis. *The Tenth International Conference on Condition Monitoring and Machinery Failure Prevention Technologies*, June 18-20, Kraków, Poland.

Machorro-López, J. M., Adams, D. E., Gómez-Mancilla, J. C., & Gul, K. A. (2009). Identification of damaged shafts using active sensing—simulation and experimentation. *Journal of Sound and Vibration*, 327(3), 368-390. doi:10.1016/j.jsv.2009.06.025

Sabnavis, G., Kirk, R. G., Kasarda, M., & Quinn, D. (2004). Cracked shaft detection and diagnostics: A literature review. *Shock and Vibration Digest*, 36(4), 287. doi:10.1177/0583102404045439

Sinou, J. J., & Lees, A. W. (2007). A non-linear study of a cracked rotor. *European Journal of Mechanics-A/Solids*, 26(1), 152-170. doi:10.1016/j.euromechsol.2006.04.002

Sinou, J. J. (2008). Detection of cracks in rotor based on the 2× and 3× super-harmonic frequency components and the crack–unbalance interactions. *Communications in Nonlinear Science and Numerical Simulation*, 13(9), 2024-2040. doi:10.1016/j.cnsns.2007.04.008

Suryawanshi, V. J., & Dhamande, L. S. (2014). Vibration Based Condition Assessment of Rotating cracked shaft using changes in critical speed and RMS Velocity response functions. *International Journal of Current Engineering and Technology*, Special Issue-3.

Varney, P., & Green, I. (2012). Crack detection in a rotor dynamic system by vibration monitoring—Part II: Extended analysis and experimental results. *Journal of Engineering for Gas Turbines and Power*, 134(11), 112501. doi:10.1115/1.4007275

Wauer, J. (1990). On the dynamics of cracked rotors: a literature survey. *Applied Mechanics Reviews*, 43(1), 13-17.

APPENDIX

Estimation of the first natural frequency of the shaft and disks.

Considering the shaft and disks only, the natural frequency of this system may be calculated as that of a mass and spring system as

$$\omega = \sqrt{\frac{m}{k}} \tag{1}$$

where m is the mass of both disks and k is the bending stiffness of the shaft. The bending stiffness of the shaft is calculated through the static deflection that the disks cause at a disk location, at a third of the shaft length or at two thirds of the shaft length. This case is illustrated in Figure 15. The solution may be obtained by a superposition of the case where a single force (F) is acted upon a beam at a random location (Budynas & Nisbett, 2011). In this case the deflection at a disk location is the superposition of two cases, one where the force acts at a third of the beam length (L), second where the force acts two thirds of the beam length. This yields the following, for the deflection at a third of the shaft length,

$$y = \frac{5}{162} \cdot \frac{FL^3}{EI} \qquad (2)$$

where y is the deflection at a disk location, E is Young's modulus and I is the shaft's second moment of inertia. The stiffness is calculated as

$$k = \frac{F}{y} \qquad (3)$$

Calculating the stiffness with the system parameters, Table 2, and substituting into Eq. (1) returns $\omega = 34.8\ Hz$.
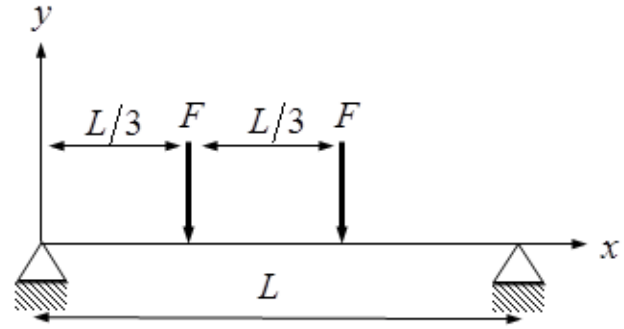
Figure 15. Simplified scheme for calculating shaft deflection due to weight of disks.

Table 2. System parameters.

Parameter	Value
Shaft diameter	20 mm
Shaft length between bearings (L)	470 mm
Young's modulus (E)	205 GPa